Volume Extreme Ultraviolet Holographic Imaging With Numerical Optical Sectioning

P. W. Wachulak, *Member, IEEE*, M. C. Marconi, *Senior Member, IEEE*, R. A. Bartels, C. S. Menoni, *Fellow, IEEE*, J. J. Rocca

NSF ERC for Extreme Ultraviolet Science & Technology and Department of Electrical and Computer Engineering, Colorado State University, Fort Collins 80521 USA

DOI: 10.1109/JPHOT.2009.XXXXXXX

Manuscript received March 3, 2008; revised November 10, 2008. First published December 10, 2008. Current version published February 25, 2009. This research was sponsored by the National Science Foundation through the NSF ERC Center for Extreme Ultraviolet Science and Technology, NSF Award No. EEC-0310717. This paper was presented in part at the National Science Foundation.

Abstract: Three dimensional images were obtained using a single high numerical aperture hologram recorded in a high resolution photoresist with a table top $\alpha = 46.9$ nm laser. Gabor holograms numerically reconstructed over a range of image planes by sweeping the propagation distance allow numerical optical sectioning that results in a robust three dimension image of a test object with a resolution in depth of approximately and a lateral resolution of 164 nm.

Index Terms: Holography, image analysis.

1. Introduction

Holographic imaging in the soft X-ray (SXR) and extreme ultraviolet (EUV) have been demonstrated in several experiments realized using EUV/SXR lasers and synchrotron sources. These include the first realization of soft X-ray laser holography at Lawrence Livermore National Laboratory using a large laser facility, and the holographic recording of biological samples and sub-micron structures using soft X-ray radiation from synchrotrons, among other experiments [1], [2]. A key idea in these experiments is to use coherent short wavelength illumination to achieve a spatial resolution beyond the reach of visible light.

Using synchrotron radiation Gabor and Fourier holograms have been demonstrated [2] with spatial resolution below 100 nm at SXR wavelengths. Compact EUV sources based on high harmonic generation (HHG) were also used to demonstrate table-top in-line EUV holography with a spatial resolution of 7.9 m and 0.8 m. Time resolved holographic imaging, that exploits the short pulsewidth of the HHG sources, was also implemented to study the ultrafast dynamics of surface deformation with a lateral resolution of the order of 100 nm [3], [5]. The recent development of compact coherent EUV laser sources, [6] has opened new opportunities for the implementation of novel imaging schemes with nanometer-scale resolution that fit on a table-top [2], [6]. In this paper, we present a proof of principle experiment in which we demonstrate that three dimensional imaging in a volume may be obtained from a single high numerical aperture (NA) hologram obtained with a table top EUV laser. Gabor holograms were numerically reconstructed over a range of image planes by sweeping the propagation distance. This numerical

sectioning technique for holography is verified to produce a robust three dimension image of a test object.

Holographic imaging in the soft X-ray (SXR) and extreme ultraviolet (EUV) have [7] been demonstrated in several experiments realized using EUV/SXR lasers and synchrotron sources. These include the first realization of soft X-ray laser holography at Lawrence Livermore National Laboratory using a large laser facility, and the holographic recording of biological samples and sub-micron structures using soft X-ray radiation from synchrotrons, among other experiments [9], [10]. A key idea in these experiments is to use coherent short wavelength illumination to achieve a spatial resolution beyond the reach of visible light [8].

Using synchrotron radiation Gabor and Fourier holograms have been demonstrated with spatial resolution below 100 nm at SXR wavelengths. Compact EUV sources based on high harmonic generation (HHG) were also used to demonstrate table-top in-line EUV holography with a spatial resolution of 7.9 m and 0.8 m. Time resolved holographic imaging, that exploits the short pulsewidth of the HHG sources, was also implemented to study the ultrafast dynamics of surface deformation with a lateral resolution of the order of 100 nm. The recent development of compact coherent EUV laser sources has opened new opportunities for the implementation of novel imaging schemes with nanometer-scale resolution that fit on a table-top. In this paper, we present a proof of principle experiment in which we demonstrate that three dimensional imaging in a volume may be obtained from a single high numerical aperture (NA) hologram obtained with a table top EUV laser. Gabor holograms were numerically reconstructed over a range of image planes by sweeping the propagation distance. This numerical sectioning technique for holography is verified to produce a robust three dimension image of a test object.

Holographic imaging in the soft X-ray (SXR) and extreme ultraviolet (EUV) have been demonstrated in several experiments realized using EUV/SXR lasers and synchrotron sources. These include the first realization of soft X-ray laser holography at Lawrence Livermore National Laboratory using a large laser facility, and the holographic recording of biological samples and sub-micron structures using soft X-ray radiation from synchrotrons, among other experiments. A key idea in these experiments is to use coherent short wavelength illumination to achieve a spatial resolution beyond the reach of visible light.

Using synchrotron radiation Gabor and Fourier holograms have been demonstrated with spatial resolution below 100 nm at SXR wavelength. Compact EUV sources based on high harmonic generation (HHG) were also used to demonstrate table-top in-line EUV holography with a spatial resolution of 7.9 m and 0.8 m. Time resolved holographic imaging, that exploits the short pulsewidth of the HHG sources, was also implemented to study the ultrafast dynamics of surface deformation with a lateral resolution of the order of 100 nm. The recent development of compact coherent EUV laser sources has opened new opportunities for the implementation of novel imaging schemes with nanometer-scale resolution that fit on a table-top. In this paper, we present a proof of principle experiment in which we demonstrate that three dimensional imaging in a volume may be obtained from a single high numerical aperture (NA) hologram obtained with a table top EUV laser. Gabor holograms were numerically reconstructed over a range of image planes by sweeping the propagation distance. This numerical sectioning technique for holography is verified to produce a robust three dimension image of a test object.

Holographic imaging in the soft X-ray (SXR) and extreme ultraviolet (EUV) have been demonstrated in several experiments realized using EUV/SXR lasers and synchrotron sources. These include the first realization of soft X-ray laser holography at Lawrence Livermore National Laboratory using a large laser facility, and the holographic recording of biological samples and sub-micron structures using soft X-ray radiation from synchrotrons, among other experiments. A key idea in these experiments is to use coherent short wavelength illumination to achieve a spatial resolution beyond the reach of visible light.

Using synchrotron radiation Gabor and Fourier holograms have been demonstrated with spatial resolution below 100 nm at SXR wavelength. Compact EUV sources based on high harmonic generation (HHG) were also used to demonstrate table-top in-line EUV holography with

a spatial resolution of 7.9 m and 0.8 m. Time resolved holographic imaging, that exploits the short pulsewidth of the HHG sources, was also implemented to study the ultrafast dynamics of surface deformation with a lateral resolution of the order of 100 nm. The recent development of compact coherent EUV laser sources has opened new opportunities for the implementation of novel imaging schemes with nanometer-scale resolution that fit on a table-top. In this paper, we present a proof of principle experiment in which we demonstrate that three dimensional imaging in a volume may be obtained from a single high numerical aperture (NA) hologram obtained with a table top EUV laser. Gabor holograms were numerically reconstructed over a range of image planes by sweeping the propagation distance. This numerical sectioning technique for holography is verified to produce a robust three dimension image of a test object.

Holographic imaging in the soft X-ray (SXR) and extreme ultraviolet (EUV) have been demonstrated in several experiments realized using EUV/SXR lasers and synchrotron sources. These include the first realization of soft X-ray laser holography at Lawrence Livermore National Laboratory using a large laser facility, and the holographic recording of biological samples and sub-micron structures using soft X-ray radiation from synchrotrons, among other experiments. A key idea in these experiments is to use coherent short wavelength illumination to achieve a spatial resolution beyond the reach of visible light.

Using synchrotron radiation Gabor and Fourier holograms have been demonstrated with spatial resolution below 100 nm at SXR wavelength. Compact EUV sources based on high harmonic generation (HHG) were also used to demonstrate table-top in-line EUV holography with a spatial resolution of 7.9 m and 0.8 m. Time resolved holographic imaging, that exploits the short pulsewidth of the HHG sources, was also implemented to study the ultrafast dynamics of surface deformation with a lateral resolution of the order of 100 nm. The recent development of compact coherent EUV laser sources has opened new opportunities for the implementation of novel imaging schemes with nanometer-scale resolution that fit on a table-top. In this paper, we present a proof of principle experiment in which we demonstrate that three dimensional imaging in a volume may be obtained from a single high numerical aperture (NA) hologram obtained with a table top EUV laser. Gabor holograms were numerically reconstructed over a range of image planes by sweeping the propagation distance.

2. Experimental Details

The experimental set up is schematically illustrated in Fig. 1. A compact $\alpha = 46.9$ nm table top discharge-pumped capillary Ne-like Ar laser occupying only a 1 ? 0.5 m2 footprint on an optical table was used for the recording of the hologram.

2.1. Some Extra Details

Lasing was obtained in the 46.9 nm 3s 1P1 ? 3p 1S0 transition of neon-like Ar by exciting Ar filled alumina capillaries 3.2 mm in diameter with a current pulse having an amplitude of 10% to 90% rise time of first half-cycle duration.

2.1.1. Even more details

The pulse generator consists of a 4 stages Marx generator charged at voltages around 45 kV. The fast current pulse was produced by discharging a water dielectric cylindrical capacitor through a spark gap switch connected in series with the capillary load. The current pulse rapidly compresses the plasma column to achieve a dense and hot filamentary plasma channel where a population inversion is created by strong monopole electron impact excitation of the laser upper level and rapid radiative relaxation of the laser lower level. The water serves as a liquid dielectric for the capacitor and also cools the capillary.

2.1.1.a. A continuous

Flow of Ar is injected in the front of the capillary and an optimum Ar gas pressure of 490 mTorr is maintained in the capillary channel. The EUV laser and the vacuum chamber where the hologram

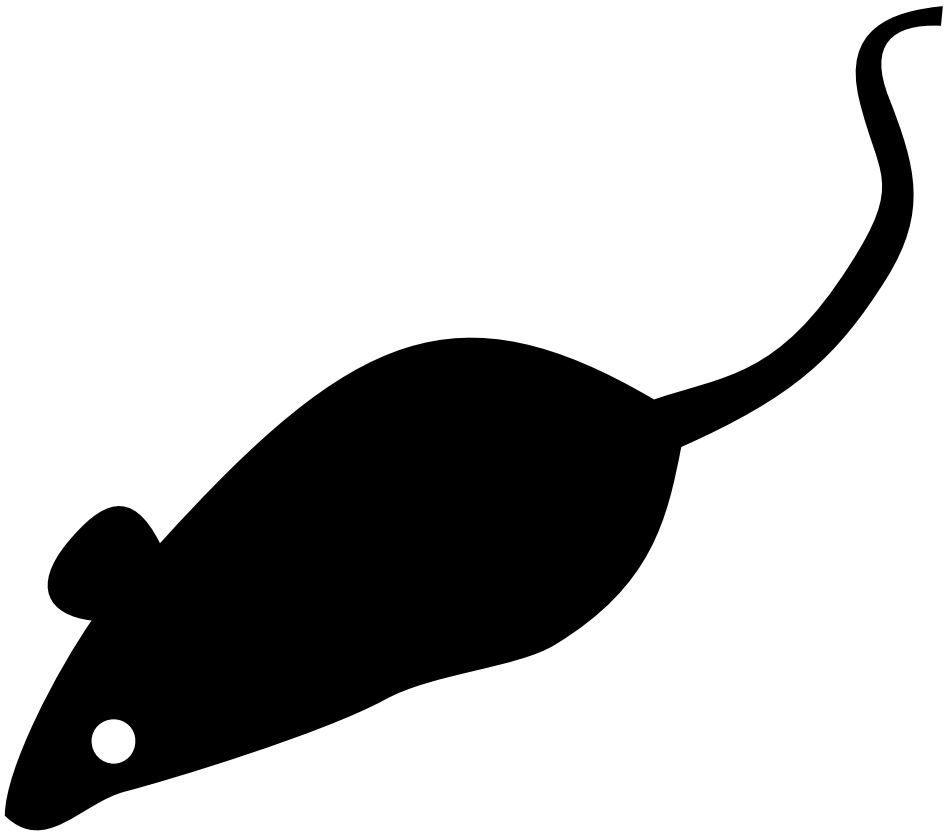

Fig. 1. (a) Diagram of the experimental set up. (b) Detail of the test object used.

was exposed, are connected via a vacuum manifold that provides differential pumping of the chamber that is maintained at 10-5 Torr. The laser, operated with 18.4 cm long capillaries, produces 0.1J pulses at a repetition rate of 1 Hz 15. The high temporal and spatial

$$x = \sum_{1=0}^{z} 2^{1} Q \tag{1}$$

coherence of the EUV table top laser permits the recording of large NA holograms for high resolution holographic imaging 18. The test object used in the holographic volume imaging experiment consisted of a tilted metallic surface covered with opaque spherical objects as can be seen in (1). This test object was fabricated placing a 100 nm thick aluminum foil covering a hole 1.5 mm in diameter made in a 80 m thick mylar sheet. The hole was partially covered with a second mylar sheet 80 m thick, as schematically indicated in Fig. 2.

Humanoid robots have received much attention recently. Although they are able to walk without falling, their movements are not natural looking. In order for these robots to move more like humans, two technological obstacles need to be addressed: Firstly, there is a lack of flexibility in their body torsos. In all human activities, movements from the spine are involved. Yet, this important factor has been neglected by the majority of humanoid robotic researchers. One of the main reasons is that the added degrees of freedom (DOF) make it more costly and difficult to build a robot. Another key issue is that it is very difficult to program these types of robots so that they can maintain balance. This numerical sectioning technique for holography is verified to produce a robust three dimension image of a test object. This numerical sectioning technique for

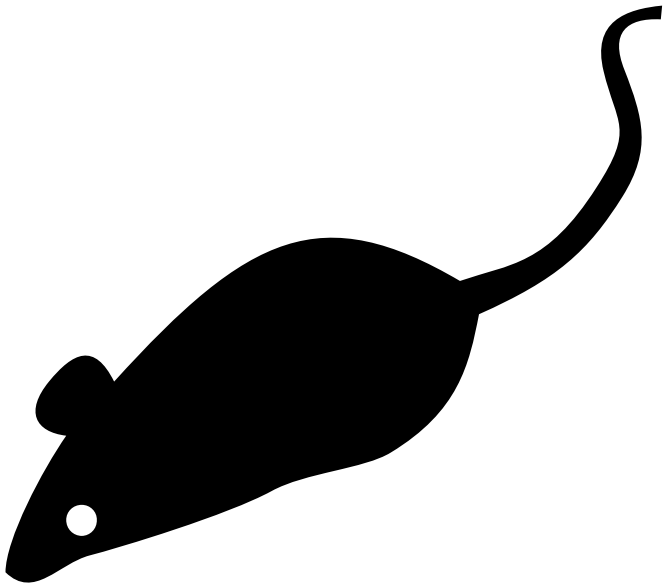

Fig. 2. Lasing was obtained in the 46.9 nm 3s 1P1 ? 3p 1S0 transition of neon-like Ar by exciting Ar filled alumina capillaries 3.2 mm in diameter with a current pulse having an amplitude Lasing was obtained in the 46.9 nm 3s 1P1 ? 3p 1S0 transition of neon-like Ar by exciting Ar filled alumina capillaries 3.2 mm in diameter with a current pulse having an amplitude

holography is verified to produce a robust three dimension image of a test object. This numerical sectioning technique for holography is verified to produce a robust three dimension image of a test object.

$$\begin{aligned} Z = {} & x_1 + x_2 + x_3 + x_4 + x_5 + x_6 \\ & + a + b \quad (2) \\ & + a + b \quad (3) \\ & + a + b \quad (4) \\ & + a + b \quad (5) \end{aligned}$$

In order to address the above technological challenges, we need to develop flexible spine humanoid robots as experimental platforms. Recently, a few researchers have developed several spinal robots based on the anatomy of the human skeleton, Mizuuchi built a tendon-driven robot called “Kenta” [1], [2]. Although the robot has a spine, there has been no data to show that it can move in a flexible way. Also, the robot cannot stand up without external support because the upper body is too heavy [2]. Mizuuchi later improved his prototype. However, it is also unable to stand up without external support [3], [5].

At the German Space Agency (DLR), Hirzinger and his group developed a spine robot called “Justin”. The robot has a 3-DOF movable upper-torso, two arms and dexterous hands. Unlike the tendon-based robots developed by Mizuuchi and his colleagues, each controllable spinal joint of Justin is directly actuated by a DC Motor via a Harmonic Drive Gear. In order to prevent the robot from falling, the designers fixed the robot to a large platform [6]. In November, 2007, researchers from Sugano Lab of Waseda University announced a new humanoid robot for household work and home care. The robot is called “Twendy-One”. It has a 4-DOF spine but it is fixed on a wheeled mobile platform. Thus, balancing is not an issue for this robot. It has a 4-DOF spine but it is fixed on a wheeled mobile platform. Thus, balancing is not an issue for this robot.

Inspired by the flexibility of belly dancers, Or conducted the first scientific study on belly dancing [7]. He developed a database of belly dancing movements using computer animations. Later, Or

TABLE I
MATH SPACINGS USED BY LATEX

Size	Width	Cmd.	Used for	Example
small	1/6 em	\,	symbols	ab
medium	2/9 em	\:	binary operators	$a+b$
large	5/18 em	\;	relational operators	$a=b$
negative small	−1/6 em	\!	misc. uses	ab

recorded the movements of a professional belly dancer using a 12-camera VICON [4] motion capture system. By analyzing the movements of the dancer, he developed a spinal mechanism which allows a full-body humanoid robot to exhibit all the human spine motions in 3D although with less degree of freedom [8]. Moreover, the robot is able to stand up while performing dynamic torso motions without external support. In terms of controlling the mechanical spine, Or used a model of the lamprey central pattern generator. Experimental results showed that by using such neural networks, only three control parameters are needed to generate all human spinal motions. In order to conduct research on human-robot interactions, Or developed a new, full-body flexible spine humanoid robot [9], [10]. Experimental results showed that it is possible for humans to perceive emotions expressed by a flexible spine humanoid robot. Later, Or developed the world's first humanoid robot that can walk more naturally, like a human, with flexible spinal motions.

The aluminum foil contours over the semicircular aperture to produce a variable height surface with the desirable characteristics for this test in Table I. The 100 nm aluminum foil has a transmission of approximately 35% at $\alpha = 46.9$ nm considering the layer of native oxide 19 and effectively cuts the lower photon energy plasma emission from the Ar discharge in the laser source. The sample was immersed in a solution of MIBK-methyl isobutyl ketone (4-Methyl-2- Pentanone) with IPA (isopropyl alcohol) 1:3 for 30 seconds, rinsed with IPA for 30 seconds, and was finally dried using compressed nitrogen $x = \sum_{1=0}^{z} 2^1 Q$.

3. Results

We adjusted the[1] exposure so that the photoresist operated in a linear response regime. With exposure by the EUV laser, the holographic interference pattern generated by the reference and the object beams was recorded in the photoresist and converted to a surface modulation after the development. Thus, the holograms were recorded as a relief pattern in the surface of a photoresist deposited on a Si wafer.

- Weight parameters for the simulated robot.
- Length of each body link.
- Specifications of body joints. Upper Torso means the spine. Due to symmetry, body parts from the right are not shown.
- Neuron parameters. Θ is the threshold, Γ is the gain. τ_D and τ_A are respectively the time constant of the dendritic sums and that of the frequency adaptation. μ is the coefficient of frequency adaptation.

Holograms recorded in such a fashion can not be reconstructed in the conventional way with an optical reconstruction beam. In order to numerically reconstruct the holograms, the surface modulation was digitized with a Novascan atomic force microscope (AFM) operated in tapping mode. Holograms recorded in such a fashion can not be reconstructed in the conventional way

[1]The aluminum foil contours over the semicircular aperture to produce a variable height surface with the desirable characteristics for this test. The 100 nm aluminum foil has a transmission of approximately 35% at $\alpha = 46.9$ nm considering the layer of native oxide 19 and effectively cuts the lower photon energy plasma emission from the Ar discharge in the laser source.

TABLE II
POSSIBLE Ω FUNCTIONS

Range	$\Omega(m)$
$x < 0$	$\Omega(m) = \sum_{i=0}^{m} K^{-i}$
$x \geq 0$	$\Omega(m) = \sqrt{m}$

TABLE III
NETWORK DELAY AS A FUNCTION OF LOAD

β	Average Delay	
	λ_{min}	λ_{max}
1	0.057	0.172
10	0.124	0.536
100	0.830	0.905*

*limited usability

with an optical reconstruction beam. In order to numerically reconstruct the holograms, the surface modulation was digitized with a Novascan atomic force microscope (AFM) operated in tapping mode.

1) Screenshot of the Webots simulation environment.
2) Schematic diagram of the simulated robot.
3) Schematic of the model lamprey CPG. Connections with a dot ending represent inhibitory connections while those with an arrow ending represent excitatory connections.
4) Sample output of a segmental oscillator (the 20th segment from the CPG). MNl and MNr respectively represents the output from the left and right motoneurons. Note the regularity of the neural pulses.

Two holograms digitized in this manner are displayed in Fig. 2. The digital reconstruction of the hologram digitized by the AFM is based on a numerical Fresnel propagator in Table II and III. To obtain the amplitude and the phase distribution of the field in the image plane, the field emerging from the hologram illuminated by a plane wave is back propagated with the Fresnel-Kirchhoff integral. The integral was evaluated by the product of the spatial frequency representation of the hologram obtained through a two dimensional fast Fourier transformation and the quadratic phase free space Fresnel propagator in the spatial frequency domain.

Theorem 1 (Einstein-Podolsky-Rosenberg):
The back-propagation distance is determined by calculating the Fresnel zone plate (FZP) focal distance for the specific hologram geometry. For the specific geometry employed in this experiment, the FZP focal length is approximately the distance between the object and the recording medium. The digital images of the holograms processed with the Fresnel propagation code generated the reconstructed images shown in Fig. 2.

Holograms recorded in such a fashion can not be reconstructed in the conventional way with an optical reconstruction beam. In order to numerically reconstruct the holograms, the surface modulation was digitized with a Novascan atomic force microscope operated in tapping mode.

Lemma 1:
The back-propagation distance is determined by calculating the Fresnel zone plate (FZP) focal distance for the specific hologram geometry For the specific geometry employed in this experiment,

the FZP focal length is approximately the distance between the object and the recording medium. The digital images of the holograms processed with the Fresnel propagation code generated the reconstructed images shown in Fig. 2.

Holograms recorded in such a fashion can not be reconstructed in the conventional way with an optical reconstruction beam. In order to numerically reconstruct the holograms.

Proof:
The back-propagation distance is determined by calculating the Fresnel zone plate (FZP) focal distance for the specific hologram geometry. For the specific geometry employed in this experiment, the FZP focal length is approximately the distance between the object and the recording medium. The digital images of the holograms processed with the Fresnel propagation code generated the reconstructed images shown in Fig. 2. ■

4. Conclusions

We have demonstrated that through detailed processing of the reconstructed holographic images, performed by changing the object-hologram distance in the reconstruction code, it is possible to discriminate depth in the object. Using a specially fabricated object composed of spherical markers 465 nm in diameter spread on a tilted transparent surface, the reconstruction and analysis of the hologram allowed to map the surface topography with a resolution close to 2 m, with such resolution depending on the particular NA of the exposure.

The lateral resolution of the image obtained by numerical reconstruction was assessed utilizing a wavelet image decomposition and image correlation. The best lateral resolution obtained with a high NA recording, 164 nm, represents an improvement of more than a factor two relative to previously published results.

Acknowledgements

The authors wish to thank the anonymous reviewers for their valuable suggestions.

References

[1] I. Mizuuchi, R. Tajima, T. Yoshikai, D. Sato, K. Nagashima, M. Inaba, Y. Kuniyoshi, and H. Inoue, "The design and control of the flexible spine of a fully tendon-driven humanoid "Kenta"," in *Proceedings of the 2002 IEEE/RSJ International Conference on Intelligent Robots and Systems*, vol. 3, Lausanne, Switzerland, 2002, pp. 2527–2532.

[2] I. Mizuuchi, H. Waita, Y. Nakanishi, T. Yoshikai, M. Inaha, and H. Inoue, "A musculo-skeletal robot leg capable of adding or rearranging the muscles," in *21th Annual Conference of the Robotics Society of Japan*. Robotics Society of Japan, Tokyo, Japan, 2003, presentation number: 1C29.

[3] I. Mizuuchi, T. Yoshiaki, Y. Nakanishi, and M. Inaba, "A reinforceable-muscle flexible-spine humanoid "Kenji"," in *IEEE/RSJ International Conference on Intelligent Robots and Systems (IROS)*, 2005, pp. 692–697.

[4] I. Mizuuchi, Y. Nakanishi, Y. Sodeyama, Y. Namiki, T. Nishino, N. Muramatsu, J. Urata, K. Hongo, T. Yoshikai, and M. Inaba, "An Advanced Musculoskeletal Humanoid Kojiro," in *Proceedings of the 2007 IEEE-RAS International Conference on Humanoid Robotics*, 2007, pp. 101–106.

[5] Y. Nakanishi, Y. Namiki, K. Hongo, J. Urata, I. Mizuuchi, and M. Inaba, "Design of the musculoskeletal trunk and realization of powerful motions using spines," in *Proceedings of the 2007 IEEE-RAS International Conference on Humanoid Robotics*, 2007, http://planning.cs.cmu.edu/humanoids07/p/85.pdf.

[6] C. Ott, O. Eiberger, W. Friedl, B. Bauml, U. Hillenbrand, C. Borst, A. Albu-Schaffer, B. Brunner, H. Hischmuller, S. Kielhofer, R. Konietschke, M. Suppa, T. Wimbock, F. Zacharias, and G. Hirzinger, "A humanoid two-arm system for dexterous manipulation," in *Proceedings of the 2006 IEEE-RAS International Conference on Humanoid Robotics*, 2006, pp. 276–283.

[7] J. Or, "A control system for a flexible spine belly dancing humanoid," *Artificial Life*, vol. 12, no. 1, pp. 63–87, 2006.

[8] J. Or and A. Takanishi, "From lamprey to humanoid: The design and control of a flexible spine belly dancing humanoid robot with inspiration from biology," *International Journal of Humanoid Robotics*, pp. 81–104, 2005.

[9] ——, "The effect of an emotional belly dancing robot on human perceptions." *International Journal of Humanoid Robotics*, vol. 4, no. 1, pp. 21–48, 2007.

[10] J. Or, "The development of emotional flexible spine humanoid robots," in *Affective Computing, Emotion Expression, Synthesis and Recognition*, J. Or, Ed. Advanced Robotics Systems, 2008.